Evidence of the Lewis-Amphoteric Character of Tris(pentafluoroethyl)silanide, [Si(C2F5)3]−

Natalia Tiessen, Mira Keßler, Beate Neumann, Hans-Georg Stammler, and Berthold Hoge

Abstract: According to a first view on the geometrical and electronic structure of the tris(pentafluoroethyl)silanide, this anion appears as a Lewis base. Quantum chemical calculations on perfluoroalkylated silanides show significantly lower HOMO and LUMO energy levels in comparison to their non-fluorinated counterparts, which implies reduced Lewis basicity and increased Lewis acidity of the [Si(C2F5)3]− ion. With these findings and a HOMO–LUMO gap of 4.80 eV similar to N-heterocyclic silylenes (NHSis), perfluoroalkyl silanides are predestined to exhibit Lewis-amphoteric character similar to silylenes. Deprotonation of Si(C2F5)3H with sterically demanding phosphazene bases afforded thermally stable phosphazenium salts of the [Si(C2F5)3]− anion, which add to benzaldehyde, benzophenone, CS2, and CO2 in various manners. This behavior also mirrors the reactivity of silylenes towards ketones as well as heterocumulenes and is rationalized by Lewis amphotericity being inherent in these silanides.

Introduction

In keeping with the Lewis definition, amphoteric species possess electron-deficient (Lewis acidic) and electron-rich (Lewis basic) centers. These reactive positions may be located on two different well separated atoms within one molecule. In a special class of Lewis-amphoteric systems, the so-called frustrated Lewis pairs (FLPs), an adduct formation is effectively prevented by sterically demanding substituents, which leads to their inherent capability to activate or incorporate a large variety of small molecules such as H_2, CO_2, CS_2, SO_2, NO_2, NO, CO, or unsaturated hydrocarbons.[1]

Yet another class of Lewis-amphoteric species derives from main group IV elements (C, Si, Ge, Sn, and Pb) in the oxidation state + II. Here, the Lewis acidic as well as the Lewis basic position are located at the same center, namely the divalent tetrel atom. The HOMO of these species displays a significant s-orbital character, whereas the LUMO is usually

represented by an empty p-orbital.[2] It is noteworthy that stable germylenes, stannylenes, and plumbylenes were long known[3] before reports on stable divalent silicon compounds as $Si(\eta^5\text{-}C_5Me_5)_2$ (Jutzi,1986)[4] or the first stable N-heterocyclic silylene [HC-NᵗBu]2Si (NHSi) (Denk & West, 1994).[5] The latter species are the higher homologues of N-heterocyclic carbenes (NHCs), the first of which has been presented by Arduengo III in 1991.[6] Denk's seminal discovery stimulated further intense research on silylene chemistry.[7–11] Due to their unique Lewis amphoteric properties, silylenes proved to be versatile and valuable building blocks in organosilicon chemistry, reacting readily with multiple bonds as present in alkenes, alkynes, ketones, imines, azides, as well as hetero-allenes X=C=Y (X, Y = O, S, NR with R = alkyl). Many of these transformations are initiated by side-on additions.[8–12] It is considered that silylenes with larger bite angles and small HOMO–LUMO gaps are more reactive than those with contrary properties.[13] Thus, for example, acyclic silylenes (HOMO–LUMO gap ca. 2 eV) can even activate H_2 affording silanes,[14] whereas NHSis cannot (HOMO–LUMO gap ca. 5 eV).[15]

Quantum chemical calculations on the tris(trifluoromethyl)silanide anion, [Si(CF3)3]−, disclose a HOMO–LUMO gap of 4.80 eV as well as lower HOMO and LUMO energy levels (−7.06 eV; −2.26 eV) in comparison to the non-fluorinated analogue, [Si(CH3)3]− (−6.88 eV; −2.10 eV) (Figure 1).[16] This is clearly due to the strong electron with-drawing effect of the perfluoroalkyl groups.[17] These computations point to a reduced Lewis basicity and in turn an increased Lewis acidity of the perfluorinated species.

Thus, we were interested in whether or not perfluoroalkyl silanides display Lewis amphoteric character similar to silylenes. To cast some light on this issue we investigated syntheses, structures, and reactivities of salts featuring the

[*] N. Tiessen, M. Keßler, B. Neumann, Dr. H.-G. Stammler, Prof. Dr. B. Hoge
Universität Bielefeld, Fakultät für Chemie
Centrum für Molekulare Materialien
Universitätsstrasse 25, 33615 Bielefeld (Germany)
E-mail: b.hoge@uni-bielefeld.de

Supporting information and the ORCID identification number(s) for the author(s) of this article can be found under:
https://doi.org/10.1002/anie.202016455.
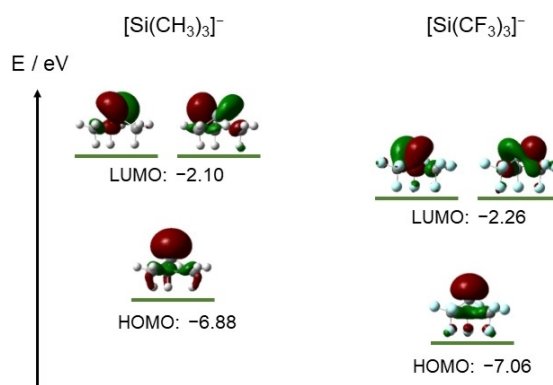
Figure 1. HOMO and LUMO energy levels of [Si(CH3)3]− and [Si(CF3)3]− (B3LYP/6-31+G(3d,p); isosurface value = 0.05 e−/au³).[16]

$[Si(C_2F_5)_3]^-$ ion and support our experimental findings by computational studies.

Results and Discussion

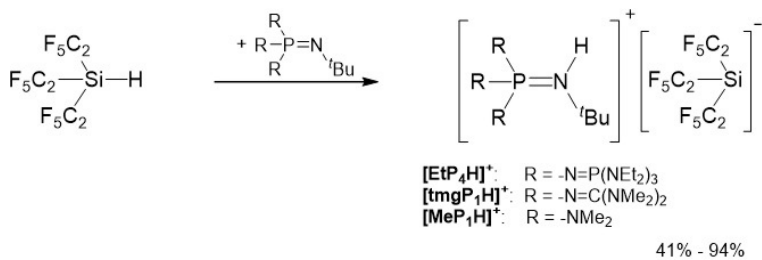While the precursor for the $[Si(C_2F_5)_3]^-$ ion, the tris(pentafluoroethyl)silane, $Si(C_2F_5)_3H$, has been originally synthesized over four steps,[18] an improved and more efficient synthesis is based upon the treatment of $SiCl_3H$ with three equivalents of in situ generated pentafluoroethyllithium, LiC_2F_5, in *n*-dibutyl ether and subsequent isothermic distillation (Scheme 1).
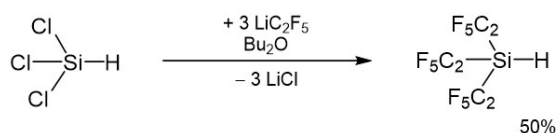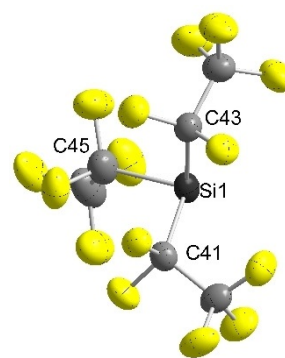
Scheme 1. Improved synthesis of $Si(C_2F_5)_3H$.

The most straightforward approach to obtain Li[Si-$(C_2F_5)_3$], the low-temperature deprotonation of Si-$(C_2F_5)_3H$[19,20] by LDA, had to be discarded due to the notorious thermolability of the product at temperatures above $-80\,°C$.[18,21] As demonstrated recently, phosphazenium cations, $[R_3P=N(H)^tBu]^+$ with R being Me_2N- ([MeP_1H]$^+$), $(Me_2N)_2C=N-$ ([$tmgP_1H$]$^+$) and $(Et_2N)_3P=N-$ ([EtP_4H]$^+$), are weakly coordinating and thus predestined to stabilize reactive anions like hydroxide trihydrate $[OH(OH_2)_3]^-$,[22] silanol silanolates,[23] or the weakly coordinating aluminate $[Al(C_2F_5)_4]^-$.[24] Consistently, deprotonation of $Si(C_2F_5)_3H$ with sterically demanding phosphazene bases $R_3P=N^tBu$ affords $[Si(C_2F_5)_3]^-$ salts in high yields (Scheme 2). The colorless products are sufficiently robust to be handled at room temperature. Elemental analyses confirm their purity (see Supporting Information).

Single crystals of $[EtP_4H][Si(C_2F_5)_3]$ were grown from a chilled solution in diethyl ether. The salt crystallizes in the triclinic space group $P\bar{1}$ with $Z = 4$ (Figure 2). One of the two symmetrically independent anions shows some disorder. Due

Figure 2. Molecular structure of the non-disordered anion in [EtP₄H]-$[Si(C_2F_5)_3]$ in the solid state.[45] Thermal ellipsoids are represented with a probability of 50%. The cation has been omitted for clarity. Selected bond lengths [pm] and angles [°] for the $[Si(C_2F_5)_3]^-$ moiety: Si1–C41 198.9(3), Si1–C43 199.6(4), Si–C45 199.6(4); C41-Si1-C43 94.8(1), C41-Si1-C45 95.8(2), C45-Si1-C43 94.0(2).

to the particularly weak interaction with the phosphazenium cation, the $[Si(C_2F_5)_3]^-$ ion is observed under so-called pseudo-gas phase conditions.[25] The C-Si-C angles of the $[Si(C_2F_5)_3]^-$ ion are significantly smaller (94.0(2)–95.8(2)°) than in the silane $Si(C_2F_5)_3H$ (107.7(3)–108.7(3)°),[18] which indicates a higher p-orbital character in the Si—C bond and a higher s-orbital character in the lone pair of the silicon atom.

Analogously to Lewis amphoteric silylenes,[26–28] the $[Si(C_2F_5)_3]^-$ ion undergoes a side-on addition with carbonyl compounds like benzaldehyde and benzophenone to afford a phosphazenium salt of the corresponding oxasiliranide anion **1a** and **1b** (Scheme 3).

[**EtP₄H**]$^+$: R = -N=P(NEt₂)₃
[**tmgP₁H**]$^+$: R = -N=C(NMe₂)₂
[**MeP₁H**]$^+$: R = -NMe₂

1a: R' = H
1b: R' = Ph
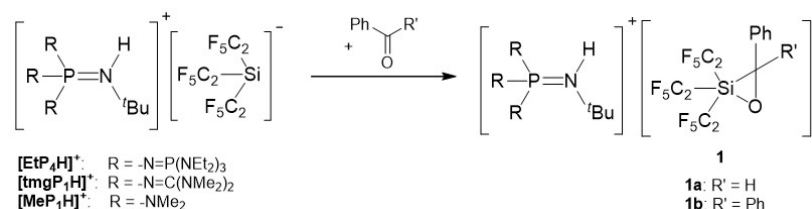
Scheme 3. Reaction of $[R_3PN(H)^tBu][Si(C_2F_5)_3]$ salts with benzaldehyde and benzophenone.

[**EtP₄H**]$^+$: R = -N=P(NEt₂)₃
[**tmgP₁H**]$^+$: R = -N=C(NMe₂)₂
[**MeP₁H**]$^+$: R = -NMe₂

41% - 94%

Scheme 2. Synthesis of several $[R_3P=N(H)^tBu][Si(C_2F_5)_3]$ salts; [$MeP_1H][Si(C_2F_5)_3]$, [$tmgP_1H][Si(C_2F_5)_3]$, and [$EtP_4H][Si(C_2F_5)_3]$.

^{29}Si NMR chemical shifts of pentafluoroethyl-substituted silicon compounds nicely correlate with the coordination number of the silicon atom and are thus useful in deducing the coordination number of the silicon atom. Thus, tetracoordinated silanes exhibit chemical shifts in the range of $+10$ to -90 ppm. Penta- and hexacoordinated pentafluoroethyl silicon compounds show chemical shifts of -95 to -150 ppm ($[SiR_5]^-$) and -150 to -200 ppm ($[SiR_6]^{2-}$), respectively.[19,20,29] In keeping with this, **1a** and **1b** feature a ^{29}Si NMR chemical shift of -127.5 ppm and -122.8 ppm, respectively. The ^{13}C NMR chemical shift of the R'PhC moiety shifts from 194.0 ppm in benzaldehyde[30a] to 75.5 ppm in **1a** and from 196.3 ppm in benzophe-

none[30b] to 78.9 ppm in **1b**. Negative ESI mass spectra reveal the molecular ion peaks of **1a** and **1b** at m/z values of 491 for $[Si(C_2F_3)_3(\eta^2\text{-CPhHO})]^-$ (**1a**) and 567 for $[Si(C_2F_5)_3(\eta^2\text{-CPh}_2O)]^-$ (**1b**).

Single crystals of [tmgP₁H]**1b** were grown by slow evaporation of a diethyl ether solution. The phosphazenium salt of $[Si(C_2F_5)_3(\eta^2\text{-CPh}_2O)]^-$ (**1b**) crystallizes in the triclinic space group $P\bar{1}$ with $Z = 4$; one of the anions is disordered. **1b** displays the geometry of a highly distorted square pyramid ($\tau = 0.18$ in the non-disordered anion and $\tau = 0.12$ in the disordered one)[31] with a C_2F_5 substituent at the apex (Figure 3). The structural motif of a three-membered Si−O−
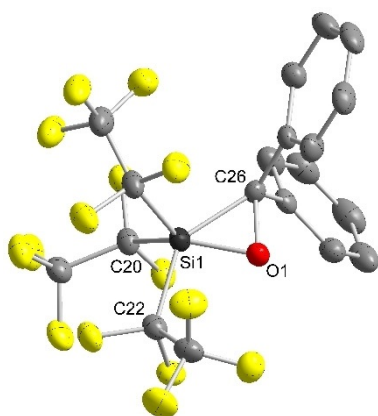

Figure 3. Molecular structure of the non-disordered anion $[Si(C_2F_5)_3(\eta^2\text{-CPh}_2O)]^-$ (**1b**) in the crystal with [tmgP₁H]⁺ as counterion.[45] Thermal ellipsoids are represented with a probability of 50%. The cation and hydrogen atoms have been omitted for clarity. Selected bond lengths [pm] and angles [°]: Si1−O1 165.5(2), C26−O1 152.0(4), Si1−C26 192.6(3); O1-Si1-C26 49.5(1), C26-O1-Si1 74.6(2), O1-C26-Si1 55.9(1).

C heterocycle is quite familiar from the side-on addition of silylenes to carbonyl compounds.[26–28] The Si1−O1 and the C26−O1 bond in the three-membered ring of **1b** are comparable to those of reported penta- and tetracoordinated oxasiliranes. The Si1−C26 bond of **1b** (192.6(3) pm) is slightly longer than in other penta- (185.0–189.2 pm)[26–28] and tetracoordinated (184.9 pm)[32] oxasiliranes. To the best of our knowledge all pentacoordinated three-membered Si−O−C-heterocycles are neutral compounds. Consequently, **1b** represents the first example of a structurally characterized negatively charged pentacoordinated oxasiliranide of type $[SiR_3(\eta^2\text{-CR}'_2O)]^-$ (R, R' = alkyl, aryl, H).

We further investigated the reaction of the $[Si(C_2F_5)_3]^-$ ion with CS₂. When [tmgP₁H][Si(C₂F₅)₃] is exposed to carbon disulfide at low temperatures, a side-on addition to CS₂ takes place. This affords the phosphazenium salt of thiasiliranide **2**, which is only stable at temperatures below −20°C (Scheme 4).

A ¹⁹F NMR spectrum of **2** at −20°C reveals signals at −79.3 ppm and −118.1 ppm for the corresponding CF₃ and the CF₂ groups. Consistent with a pentacoordinated silicon atom, **2** features a ²⁹Si NMR chemical shift of −102.6 ppm.

When [tmgP₁H][Si(C₂F₅)₃(η²-CS₂)] was generated in situ at −40°C and *n*-hexane was slowly diffused into the solution,
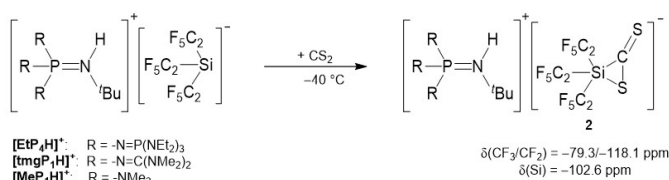
Scheme 4. Reaction of $[R_3PN(H)^tBu][Si(C_2F_5)_3]$ with CS₂.

single crystals were obtained, which were prepared at low temperatures for X-ray diffraction analysis. [tmgP₁H][Si-(C₂F₅)₃(η²-CS₂)] crystallizes in the monoclinic space group $P2_1/n$; two C_2F_5 groups are disordered over two sites. Thiasiliranide **2** exhibits a highly distorted geometry with rather a trigonal-bipyramidal than a square-pyramidal geometry ($\tau = 0.51$, Figure 4). The Si1−S1 bond (266.0(1) pm) is
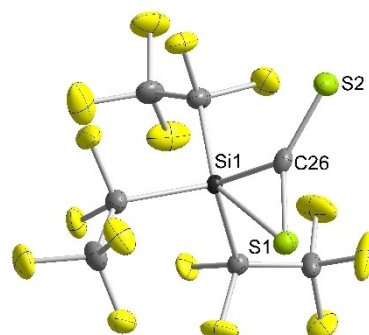
Figure 4. Molecular structure of $[Si(C_2F_5)_3(\eta^2\text{-CS}_2)]^-$ (**2**) in the solid state with [tmgP₁H]⁺ as counterion.[45] Thermal ellipsoids are represented with a probability of 50%. The cation and minor occupied disordered C_2F_5 groups have been omitted for clarity. Selected bond lengths [pm] and angles [°]: Si1−S1 266.0(1), Si1−C26 184.3(2), C26−S1 169.6(2), C26−S2 165.3(2); C26-Si1-S1 39.2(1), Si1-S1-C26 43.4(1), Si1-C26-S1 97.4(1), Si1-C26-S2 131.1(1), S1-C26-S2 131.5(1).

significantly longer than in tetracoordinated thiasilirane **I** (209.3 pm)[33] and 10 pm longer than in pentacoordinated thiasiliranide ion **II** (256.9(9) pm, Figure 5).[34] However, the Si1−S1 bond is much shorter than the sum of the van der Waals radii (390 pm),[35] which implies some degree of silicon−sulfur bonding. Surprisingly, the C26−S2 bond (165.3-(2) pm) is only about 4 pm shorter than the C26−S1 bond (169.6(2) pm) and both are in the range of typical C=S double bonds (ca. 167 pm).[36] This bond situation is also observed in η²-CS₂ transition metal complexes (e.g. 163.3 and 169.3 pm in **III**).[37] In comparison, C=S bonds in crystallized CS₂ are about 154 pm.[38]
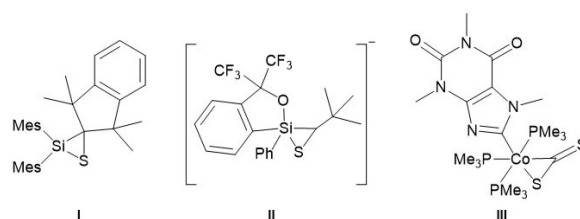
Figure 5. Thiasilirane **I**, thiasiliranide ion **II**, and η²-CS₂ complex **III**.

Since CO_2 is one of the main greenhouse gases known, enormous efforts have been made to capture, store, and activate CO_2 for the synthesis of value-added products. Apart from transition metal complexes,[39] some silylenes are known to successfully activate CO_2.[40] Most silylenes form dimeric species like, for example, **IV**,[41] whereas only a few of them lead to compounds like **V–VIII** with chelating carbonate ligands (Figure 6).[42]
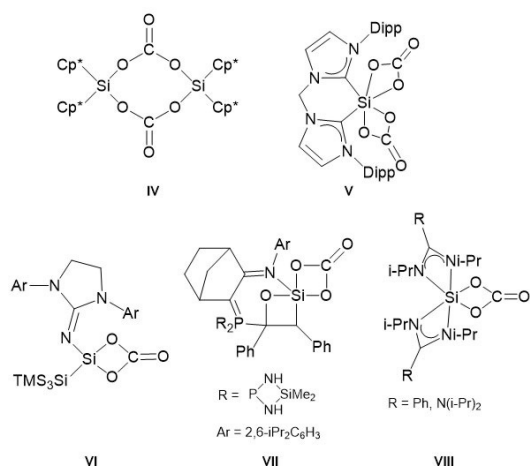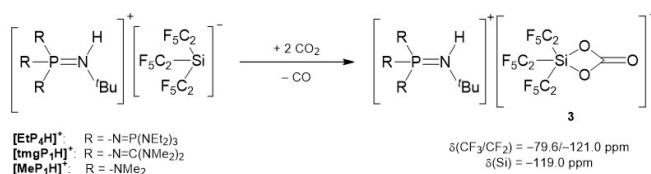
Figure 6. Examples of known silicon carbonates.

When a $[Si(C_2F_5)_3]^-$ salt is treated with an excess of CO_2, the corresponding salt of silicon carbonate **3** is formed (Scheme 5). The formation of CO was monitored by IR spectroscopy of the gas phase.

Scheme 5. Reaction of $[R_3PN(H)^tBu][Si(C_2F_5)_3]$ with CO_2.

The ^{19}F NMR spectrum of **3** reveals signals at -79.6 ppm and -121.0 ppm resulting from the CF_3 and CF_2 groups. In accordance with a pentacoordinated silicon center, **3** features a resonance at -119.0 ppm in the ^{29}Si NMR spectrum. The carbonyl carbon atom resonates in the ^{13}C NMR spectrum at 148.6 ppm. In the IR spectrum, the $\tilde{\nu}(C=O)$ mode is detected at 1703 cm^{-1}.

Upon evaporation of the solvent, decomposition of **3** to $[(F_5C_2)CO_2]^-$ and other unidentified species occurs. Nevertheless single crystals of $[EtP_4H][Si(C_2F_5)_3(\eta^2-CO_3)]$ were obtained by diffusion of *n*-heptane in a Et_2O/THF solution of the silicon carbonate salt at $-40\,°C$. $[EtP_4H][Si(C_2F_5)_3(\eta^2-CO_3)]$ crystallizes in the monoclinic space group $P2_1/c$ (Figure 7). Silicon carbonate **3** exhibits a highly distorted geometry with a slight tendency to a trigonal bipyramid ($\tau = 0.53$). The Si1−O2 bond (181.5(2) pm) is about 11 pm longer than the Si1−O1 bond (170.1(2) pm). Both Si−O bond lengths are
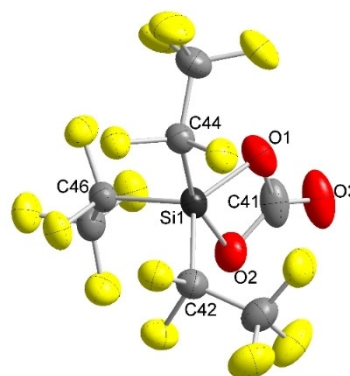

Figure 7. Molecular structure of the $[Si(C_2F_5)_3(\eta^2-CO_3)]^-$ anion (**3**) in the solid state with $[EtP_4H]^+$ as counterion.[45] Thermal ellipsoids are represented with a probability of 50%. The cation has been omitted for clarity. Selected bond lengths [pm] and angles [°]: Si1–O1 170.1(2), Si1–O2 181.5(2), C41–O3 119.1(4); O1-Si1-O2 73.8(1), O2-C41-O1 103.6(3), O3-C41-O1 126.5(4), O2-C41-O3 129.8(4).

in the range of known silicon carbonates (171.5–180.4 pm).[40,41] The C41=O3 bond length is comparable to the ones in other silicon carbonates, underlining its double-bond character. The sum of the angles about C41 of 359.9° confirms a planar coordination sphere. Though some silicon carbonates are known, to the best of our knowledge **3** represents the first structurally characterized negatively charged silicon carbonate of the type $[SiR_3(\eta^2-CO_3)]^-$ with exclusively organic substituents R = aryl, alkyl.

Computational Studies

In order to support our experimental findings, we performed computational studies at B3LYP/6-31 + G(3d,p) level of theory[16] concerning the mechanism of the side-on addition of the tris(trifluoromethyl)silanide ion, $[Si(CF_3)_3]^-$, to formaldehyde, benzaldehyde, benzophenone, and CS_2 as well as of the reaction with CO_2. To reduce computational cost, electronically similar trifluoromethyl groups instead of pentafluoroethyl groups were used. For the same reason we only investigated the addition of formaldehyde in more detail. For each depicted transition state an intrinsic reaction coordinate calculation was performed to ensure that they indeed connect the correct minima. Further details are given in the Supporting Information.

The addition of formaldehyde to $[Si(CF_3)_3]^-$ is a concerted process leading to the product $[Si(CF_3)_3(\eta^2-CH_2O)]^-$. Figure 8 shows a distortion/interaction diagram[43] for the reaction path in relation to the Si–C$_{formaldehyde}$ distance. Unsurprisingly, the energy required for distortion of the reactants increases with decreasing distance. For values above 265 pm the interaction energy between the fragments outweighs the energy required for distortion due to long-range interactions of the negatively charged silanide and the dipole of formaldehyde. We located a weakly bound complex as a minimum with a Si–C distance of 367 pm and a change in electronic energy (ΔE, zero-point corrected) of -21.3 kJ mol^{-1} relative to the starting com-
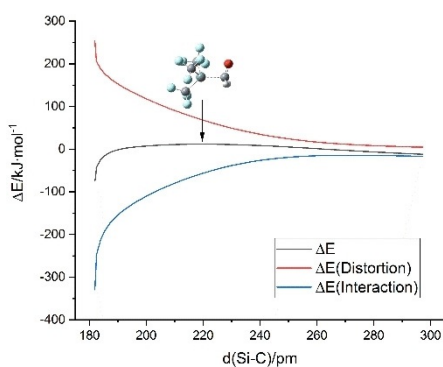
Figure 8. Distortion/interaction diagram of the reaction path of [Si-$(CF_3)_3$]$^-$ + CH_2O in relation to the Si–$C_{formaldehyde}$ distance. The change in energy is given relative to the starting compounds. The transition state is marked with an arrow.

pounds. However, the change in Gibbs free energy (ΔG, Figure 9) is $+6.0 \, kJ \, mol^{-1}$, indicating that this complex has very little influence on the outcome of the reaction.
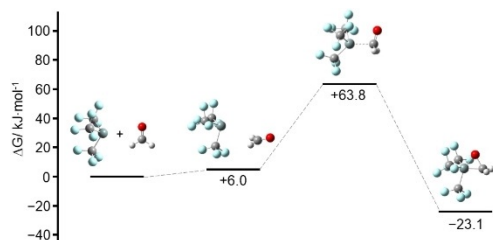
Figure 9. Change in Gibbs free energy along the reaction pathway of [Si$(CF_3)_3$]$^-$ + CH_2O.

Furthermore, we performed an NBO analysis[44] of the silanide as well as of the transition state. In [Si$(CF_3)_3$]$^-$ the highest Lewis-NBO is the lone pair at the silicon atom (occupancy: 1.92) and the lowest non-Lewis-NBOs are antibonding and located at the Si–C bonds (occupancy: 0.05 each). The transition state is best described as an alcoholate with a Si–$C_{formaldehyde}$ bond. However, the occupancy of the three lone pairs at the oxygen atom is relatively low (1.62, 1.88, and 1.98), whereas the antibonding Si–$C_{formaldehyde}$ (0.33) is relatively highly occupied due to an extremely large stabilization value from delocalization of one lone pair into this antibonding Si–C NBO (256.6 $kJ \, mol^{-1}$). The antibonding Si–$C_{trifluoromethyl}$ NBOs have higher occupancies than the corresponding ones in [Si$(CF_3)_3$]$^-$ (anti-periplanar to O: 0.15, synclinal to O: 0.08 each). Delocalization of the lone pairs at the oxygen atom into the Si–C antibond in *trans* position has stabilization values of 7.1 $kJ \, mol^{-1}$ and 3.1 $kJ \, mol^{-1}$.

In contrast to the perfluorinated silanide, the non-fluorinated [Si$(CH_3)_3$]$^-$ ion attacks only the carbon atom of formaldehyde, forming [Si$(CH_3)_3(\eta^1$-$CH_2O)$]$^-$ (Figure 10). [Si$(CH_3)_3(\eta^2$-$CH_2O)$]$^-$ is 82.1 $kJ \, mol^{-1}$ higher in energy and therefore immaterial to the reaction. Since no transition state between the starting compounds and [Si$(CH_3)_3(\eta^1$-$CH_2O)$]$^-$ was found, we performed a relaxed potential energy scan
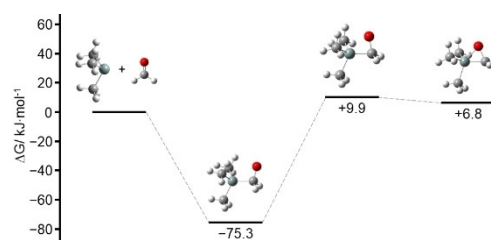
Figure 10. Change in Gibbs free energy along the reaction pathway of [Si$(CH_3)_3$]$^-$ + CH_2O.

along the Si–$C_{formaldehyde}$ bond to gain some insight into the reaction path (Figure 11). Apparently, it is a highly exothermic reaction with no activation barrier.
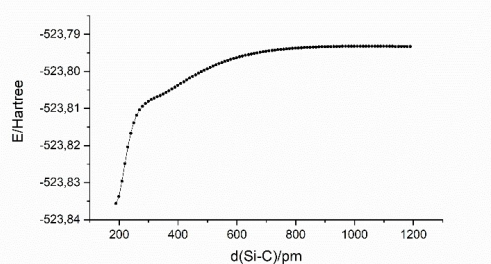
**Figure 11.** Plot of the electronic energy in relation to the Si–$C_{formaldehyde}$ distance obtained by a relaxed potential energy scan.

The addition of [Si$(CF_3)_3$]$^-$ to benzaldehyde, benzophenone, and CS_2 proceeds analogously to the reaction with formaldehyde. The reaction parameters are given in Table 1. The activation barrier of the addition to the bulkier benzaldehyde is higher than of the addition to formaldehyde. The addition to benzophenone has the highest activation barrier. Since the reaction time was by far the longest, this is consistent with the experimental results. The ΔG value is positive, which contradicts the experiment, but those values are known to be error-prone.

Contrary to the other reactions, CO_2 does not add side-on in a concerted mechanism to [Si$(CF_3)_3$]$^-$. Stationary points are shown in Figure 12. Although we located two local energy minima along the reaction pathway, [Si$(CF_3)_3(\eta^1$-$CO_2)$]$^-$ and

Table 1: Change in energy (zero-point corrected) and Gibbs free energy (298.15 K, 1.0 atm) for the transition state ($\Delta E^{\ddagger}$ and $\Delta G^{\ddagger}$) and the product (ΔE and ΔG) of the concerted side-on addition of [Si$(CF_3)_3$]$^-$ to formaldehyde, benzaldehyde, benzophenone, and CS_2.

Substrate	$\Delta E^{\ddagger}$(TS) [kJ mol^{-1}]	ΔE(Product) [kJ mol^{-1}]	$\Delta G^{\ddagger}$(TS) [kJ mol^{-1}]	ΔG(Product) [kJ mol^{-1}]
CH_2O	17.9	−71.1	63.8	−23.1
CPhHO	38.2	−59.7	90.7	−4.4
CPh$_2$O	58.4	−45.5	115.3	9.9
CS_2[a]	37.2	−52.3	70.0	−7.9

[a] Note that the reaction was carried out at temperatures below −20 °C due to decomposition of the product, but ΔG is given for room temperature.
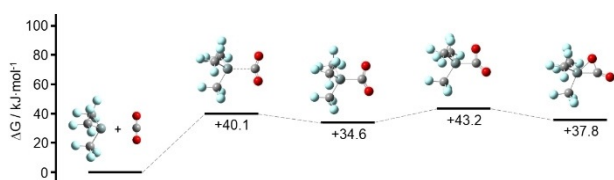
Figure 12. Change in Gibbs free energy along the reaction pathway of $[Si(CH_3)_3]^- + CO_2$.

$[Si(CF_3)_3(\eta^2\text{-}CO_2)]^-$, ΔG is positive in both cases, suggesting that these are not the favored products. Based on the experimental results we studied potential consecutive reactions. One possible reaction starts with the elimination of CO from $[Si(CF_3)_3(\eta^2\text{-}CO_2)]^-$ followed by the addition of a second equivalent of CO_2 (Figure 13). However, since $[Si(CF_3)_3(\eta^2\text{-}$
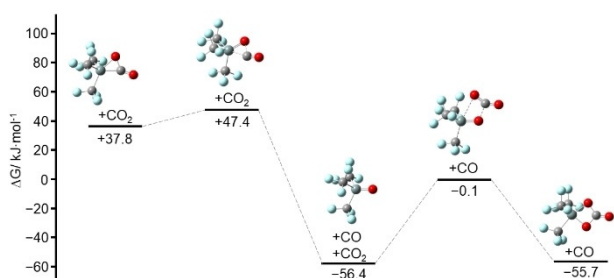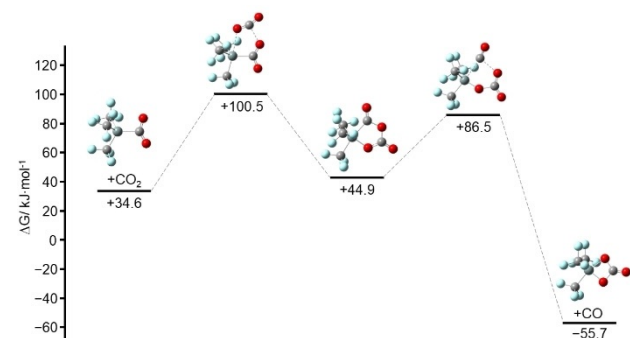

Figure 13. Change in Gibbs free energy along one possible reaction pathway of $[Si(CF_3)_3(\eta^2\text{-}CO_2)]^- + CO_2$ relative to the initial educts.

$CO_3)]^-$ is 0.7 kJ mol^{-1} higher in energy than $[Si(CF_3)_3O]^- + CO_2$ this pathway seems not likely. Another possibility starts with the addition of a second equivalent CO_2 to $[Si(CF_3)_3(\eta^1\text{-}CO_2)]^-$, forming an intermediate product featuring a five-membered ring (Figure 14). In this case elimination of CO would lead to the overall thermodynamically favored product $[Si(CF_3)_3(\eta^2\text{-}CO_3)]^-$.

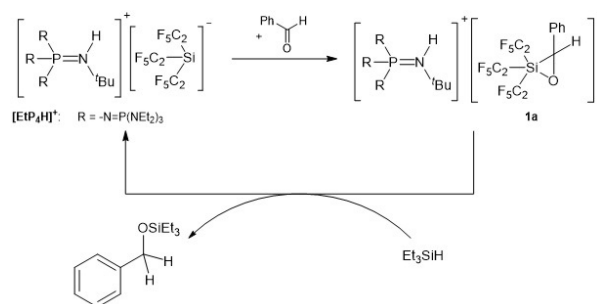***Figure 14.*** Change in Gibbs free energy along one possible reaction pathway of $[Si(CF_3)_3(\eta^1\text{-}CO_2)]^- + CO_2$ relative to the initial starting compounds.

Conclusion

In this Research Article we reported on high yielding (up to 94%) syntheses of room-temperature stable $[Si(C_2F_5)_3]^-$ salts utilizing phosphazenium cations, which as weakly

coordinating cations stabilize the reactive anion. This allows the structural characterization of the anion under so-called pseudo-gas phase conditions. Most importantly, while exploring the reactivity of the $[Si(C_2F_5)_3]^-$ ion we disclosed its formal Lewis amphoteric behavior. Just like silylenes, the anion displays Lewis basic and Lewis acidic character. This is evident by the side-on additions to benzaldehyde, benzophenone, and CS_2, as well as by the activation of CO_2. We isolated and structurally characterized novel negatively charged species like oxasiliranide **1b**, thiasiliranide **2**, and silicon carbonate **3**. To the best of our knowledge, **1b** and **3** represent the first examples of structurally characterized negatively charged hypervalent three- and four-membered heterocycles $[R_3Si(\eta^2\text{-}CR'_2O)]^-$ and $[R_3Si(\eta^2\text{-}CO_3)]^-$ (R, R' = alkyl, aryl, H) with organic substituents. Preliminary investigations show that the tris(pentafluoroethyl)silanide catalyzes hydrosilylation of carbonyl compounds like benzaldehyde with triethylsilane via the herein isolated oxasiliranide **1a** (Scheme 6). Detailed studies concerning this hydrosilylation and the activation of other small molecules by $[Si(C_2F_5)_3]^-$ are in progress.

Scheme 6. Catalytic hydrosilylation of benzaldehyde by [EtP$_4$H][Si(C$_2$F$_5$)$_3$] via [EtP$_4$H]**1a**.

Conflict of interest

The authors declare no conflict of interest.

[1] a) D. W. Stephan, G. Erker, *Frustrated Lewis Pairs I: Uncovering and Understanding*, Springer, Heidelberg, **2013**; b) D. W. Stephan, G. Erker, *Frustrated Lewis Pairs II,: Expanding the Scope*, Springer, Heidelberg, **2013**; c) D. W. Stephan, *Science* **2016**, *354*, aaf7229; d) D. W. Stephan, G. Erker, *Angew. Chem. Int. Ed.* **2015**, *54*, 6400; *Angew. Chem.* **2015**, *127*, 6498.

[2] K. Klinkhammer, *Polyhedron* **2002**, *21*, 587.

[3] a) N. Tokitoh, R. Okazaki, *Coord. Chem. Rev.* **2000**, *210*, 251; b) W. P. Neumann, *Chem. Rev.* **1991**, *91*, 311; c) J. Satgé, M. Massol, P. Rivière, *J. Organomet. Chem.* **1973**, *56*, 1; d) M. F. Lappert, *Main Group Met. Chem.* **1994**, *17*, 183.

[4] P. Jutzi, D. Kanne, C. Krüger, *Angew. Chem.* **1986**, *98*, 163.

[5] M. Denk, R. Lennon, R. Hayashi, R. West, A. V. Belyakov, H. P. Verne, A. Haaland, M. Wagner, N. Metzler, *J. Am. Chem. Soc.* **1994**, *116*, 2691.

[6] A. J. Arduengo, R. L. Harlow, M. Kline, *J. Am. Chem. Soc.* **1991**, *113*, 361.

[7] a) M. Haaf, A. Schmiedl, T. A. Schmedake, D. R. Powell, A. J. Millevolte, M. Denk, R. West, *J. Am. Chem. Soc.* **1998**, *120*, 12714; b) M. Haaf, T. A. Schmedake, R. West, *Acc. Chem. Res.* **2000**, *33*, 704; c) B. Gehrhus, M. F. Lappert, *J. Organomet. Chem.* **2001**, *617*, 209; d) R. Tacke, T. Ribbeck, *Dalton Trans.* **2017**, *46*, 13628; e) S. Raoufmoghaddam, Y.-P. Zhou, Y. Wang, M. Driess, *J. Organomet. Chem.* **2017**, *829*, 2; f) *Organosilicon Compounds. Theory and Experiment (Synthesis)* (Ed.: V. Y. Lee), Elsevier, Amsterdam, **2017**.

[8] N. J. Hill, R. West, *J. Organomet. Chem.* **2004**, *689*, 4165.

[9] H. W. Roesky, *J. Organomet. Chem.* **2013**, *730*, 57.

[10] S. Yao, Y. Xiong, M. Driess, *Organometallics* **2011**, *30*, 1748.

[11] M. Asay, C. Jones, M. Driess, *Chem. Rev.* **2011**, *111*, 354.

[12] a) S. S. Sen, S. Khan, S. Nagendran, H. W. Roesky, *Acc. Chem. Res.* **2012**, *45*, 578; b) W. H. Atwell, *Organometallics* **2009**, *28*, 3573; c) Y. Mizuhata, T. Sasamori, N. Tokitoh, *Chem. Rev.* **2009**, *109*, 3479.

[13] C. Shan, S. Yao, M. Driess, *Chem. Soc. Rev.* **2020**, *49*, 6733.

[14] a) M. Driess, *Nat. Chem.* **2012**, *4*, 525; b) A. V. Protchenko, K. H. Birjkumar, D. Dange, A. D. Schwarz, D. Vidovic, C. Jones, N. Kaltsoyannis, P. Mountford, S. Aldridge, *J. Am. Chem. Soc.* **2012**, *134*, 6500; c) A. V. Protchenko, A. D. Schwarz, M. P. Blake, C. Jones, N. Kaltsoyannis, P. Mountford, S. Aldridge, *Angew. Chem. Int. Ed.* **2013**, *52*, 568; *Angew. Chem.* **2013**, *125*, 596.

[15] U. Radius, J. Nitsch, M. J. Krahfuß, F. M. Bickelhaupt, T. B. Marder, *Chem. Eur. J.* **2020**, *26*, 11276.

[16] M. J. Frisch, G. W. Trucks, H. B. Schlegel, G. E. Scuseria, M. A. Robb, J. R. Cheeseman, G. Scalmani, V. Barone, B. Mennucci, G. A. Petersson, H. Nakatsuji, M. Caricato, X. Li, H. P. Hratchian, A. F. Izmaylov, J. Bloino, G. Zheng, J. L. Sonnenberg, M. Hada, M. Ehara, K. Toyota, R. Fukuda, J. Hasegawa, M. Ishida, T. Nakajima, Y. Honda, O. Kitao, H. Nakai, T. Vreven, J. A. Montgomery, Jr., J. E. Peralta, F. Ogliaro, M. Bearpark, J. J. Heyd, E. Brothers, K. N. Kudin, V. N. Staroverov, T. Keith, R. Kobayashi, J. Normand, K. Raghavachari, A. Rendell, J. C. Burant, S. S. Iyengar, J. Tomasi, M. Cossi, N. Rega, J. M. Millam, M. Klene, J. E. Knox, J. B. Cross, V. Bakken, C. Adamo, J. Jaramillo, R. Gomperts, R. E. Stratmann, O. Yazyev, A. J. Austin, R. Cammi, C. Pomelli, J. W. Ochterski, R. L. Martin, K. Morokuma, V. G. Zakrzewski, G. A. Voth, P. Salvador, J. J. Dannenberg, S. Dapprich, A. D. Daniels, O. Farkas, J. B. Foresman, J. V. Ortiz, J. Cioslowski, D. J. Fox, *Gaussian 09, Revision D.01*, Gaussian, Inc., Willingford CT, **2013**.

[17] S. Elbel, H. T. Dieck, R. Demuth, *J. Fluorine Chem.* **1982**, *19*, 349.

[18] N. Schwarze, S. Steinhauer, B. Neumann, H.-G. Stammler, B. Hoge, *Angew. Chem. Int. Ed.* **2016**, *55*, 16156; *Angew. Chem.* **2016**, *128*, 16390.

[19] S. Steinhauer, H.-G. Stammler, B. Neumann, N. Ignat'ev, B. Hoge, *Angew. Chem. Int. Ed.* **2014**, *53*, 562; *Angew. Chem.* **2014**, *126*, 573.

[20] S. Steinhauer, J. Bader, H.-G. Stammler, N. Ignat'ev, B. Hoge, *Angew. Chem. Int. Ed.* **2014**, *53*, 5206; *Angew. Chem.* **2014**, *126*, 5307.

[21] N. Schwarze, S. Steinhauer, B. Neumann, H.-G. Stammler, B. Hoge, *Angew. Chem. Int. Ed.* **2016**, *55*, 16161; *Angew. Chem.* **2016**, *128*, 16395.

[22] R. F. Weitkamp, B. Neumann, H.-G. Stammler, B. Hoge, *Angew. Chem. Int. Ed.* **2019**, *58*, 14633; *Angew. Chem.* **2019**, *131*, 14775.

[23] R. F. Weitkamp, B. Neumann, H.-G. Stammler, B. Hoge, *Angew. Chem. Int. Ed.* **2020**, *59*, 5494; *Angew. Chem.* **2020**, *132*, 5536.

[24] N. Tiessen, B. Neumann, H.-G. Stammler, B. Hoge, *Chem. Eur. J.* **2020**, *26*, 13611.

[25] I. Krossing, A. Reisinger, *Coord. Chem. Rev.* **2006**, *250*, 2721.

[26] R. S. Ghadwal, S. S. Sen, H. W. Roesky, M. Granitzka, D. Kratzert, S. Merkel, D. Stalke, *Angew. Chem. Int. Ed.* **2010**, *49*, 3952; *Angew. Chem.* **2010**, *122*, 4044.

[27] R. Azhakar, R. S. Ghadwal, H. W. Roesky, J. Hey, D. Stalke, *Organometallics* **2011**, *30*, 3853.

[28] D. Gau, R. Rodriguez, T. Kato, N. Saffon-Merceron, F. P. Cossío, A. Baceiredo, *Chem. Eur. J.* **2010**, *16*, 8255.

[29] a) S. Steinhauer, T. Böttcher, N. Schwarze, B. Neumann, H.-G. Stammler, B. Hoge, *Angew. Chem. Int. Ed.* **2014**, *53*, 13269; *Angew. Chem.* **2014**, *126*, 13485; b) N. Schwarze, B. Kurscheid, S. Steinhauer, B. Neumann, H.-G. Stammler, N. Ignat'ev, B. Hoge, *Chem. Eur. J.* **2016**, *22*, 17460.

[30] a) H. M. Maurer, J. Bargon, *J. Am. Chem. Soc.* **1979**, *101*, 6865; b) A. W. Frahm, H. F. Hambloch, *Org. Magn. Reson.* **1980**, *14*, 444.

[31] A. W. Addison, T. N. Rao, *J. Chem. Soc. Dalton Trans.* **1984**, 1349.

[32] a) W. Ando, Y. Hamada, A. Sekiguchi, *Tetrahedron Lett.* **1982**, *23*, 5323; b) S. Ishida, T. Iwamoto, M. Kira, *Organometallics* **2010**, *29*, 5526; c) H.-J. Liu, C. Landis, C. Raynaud, O. Eisenstein, T. D. Tilley, *J. Am. Chem. Soc.* **2015**, *137*, 9186.

[33] W. Ando, Y. Hamada, A. Sekiguchi, *Tetrahedron Lett.* **1983**, *24*, 4033.

[34] K. Naganuma, T. Kawashima, *J. Organomet. Chem.* **2002**, *643–644*, 504.

[35] S. S. Batsanov, *Inorg. Mater.* **2001**, *37*, 871.

[36] F. H. Allen, O. Kennard, D. G. Watson, L. Brammer, A. G. Orpen, R. Taylor, *J. Chem. Soc. Perkin Trans. 2* **1987**, S1–S19.

[37] T. Zheng, W. Xu, J. Li, F. Lu, *Z. Kristallogr. New Cryst. Struct.* **2013**, *228*, 189.

[38] V. V. Kveder, E. A. Steinman, B. Z. Narymbetov, S. S. Khasanov, L. P. Rozenberg, R. P. Shibaeva, A. V. Bazhenov, A. V. Gorbunov, M. Y. Maksimuk, D. V. Konarev, R. N. Lyubovskaya, Y. A. Ossipyan, *Chem. Phys.* **1997**, *216*, 407.

[39] a) T. Sakakura, J.-C. Choi, H. Yasuda, *Chem. Rev.* **2007**, *107*, 2365; b) Q. Liu, L. Wu, R. Jackstell, M. Beller, *Nat. Commun.* **2015**, *6*, 5933.

[40] a) Y. Wang, M. Chen, Y. Xie, P. Wei, H. F. Schaefer, G. H. Robinson, *J. Am. Chem. Soc.* **2015**, *137*, 8396; b) X. Liu, X.-Q. Xiao, Z. Xu, X. Yang, Z. Li, Z. Dong, C. Yan, G. Lai, M. Kira, *Organometallics* **2014**, *33*, 5434.

[41] P. Jutzi, D. Eikenberg, A. Möhrke, B. Neumann, H.-G. Stammler, *Organometallics* **1996**, *15*, 753.

[42] a) R. Rodriguez, I. Alvarado-Beltran, J. Saouli, N. Saffon-Merceron, A. Baceiredo, V. Branchadell, T. Kato, *Angew. Chem. Int. Ed.* **2018**, *57*, 2635; *Angew. Chem.* **2018**, *130*, 2665; b) A. Burchert, S. Yao, R. Müller, C. Schattenberg, Y. Xiong, M. Kaupp, M. Driess, *Angew. Chem. Int. Ed.* **2017**, *56*, 1894; *Angew. Chem.* **2017**, *129*, 1920; c) D. Wendel, A. Porzelt, F. A. D. Herz, D. Sarkar, C. Jandl, S. Inoue, B. Rieger, *J. Am. Chem. Soc.* **2017**, *139*, 8134; d) F. M. Mück, J. A. Baus, M. Nutz, C. Burschka, J.

Poater, F. M. Bickelhaupt, R. Tacke, *Chem. Eur. J.* **2015**, *21*, 16665; e) K. Junold, M. Nutz, J. A. Baus, C. Burschka, C. Fonseca Guerra, F. M. Bickelhaupt, R. Tacke, *Chem. Eur. J.* **2014**, *20*, 9319.

[43] F. M. Bickelhaupt, K. N. Houk, *Angew. Chem. Int. Ed.* **2017**, *56*, 10070; *Angew. Chem.* **2017**, *129*, 10204.

[44] E. D. Glendining, J. K. Badenhoop, A. E. Reed, J. E. Carpenter, J. A. Bohmann, C. M. Morales, C. R. Landis, F. Weinhold, *NBO*

6.0, Theoretical Chemistry Institute, University of Wisconsin, Madison, WI, **2013**.

[45] CCDC 2005658, 2005659, 2005660 and 2027760.